Deliverable Name: Final results on proposed ESH-friendly cleaning methods of low-k dielectrics; final ESH impact results
Task ID: 425.022
Task Title: Environmentally-Friendly Cleaning of New Materials and Structures for Future Micro- and Nano-Electronics Manufacturing

Summary/Abstract

Owing to the recent extensive development of high-k dielectric technologies, the interface property of Ge and III-V semiconductor gate stack have been greatly improved. In this work, we investigated key interface engineering for Ge and III-V semiconductor gate stack: GeO_2 interfacial layer and interface self-cleaning effect in III-V semiconductor during Atomic Layer Deposition process of high-k dielectric films, by electrical characterization and photoemission spectroscopy. GeO_2 interfacial layer significantly improves interface property of high-k/Ge stack and self-cleaning effect in high-k/III-V semiconductor stack provides native oxide free interface which will result in Fermi-level unpinning.

(1) **GeO2 interfacial layer in high-k dielectri/Ge stack:** We utilized radical oxidation for high quality GeO_2 growth. Fig. 1 shows the kinetics curve of GeO_2 growth on (100) and (111) Ge substrates. There is no orientation dependence of GeO_2 growth, which is an advantage when fabricating non-planer Ge MOSFET. Fig. 2 shows typical Ge 3d core level spectra of thermally and plasma oxidized Ge substrate. Radical oxidation provides stoichiometric GeO_2 growth and identical spectrum for (100) and (111) Ge substrate. Fig. 3 shows temperature dependence of GeO_2 growth rate. Radical oxidation has smaller temperature dependence which will provide small thickness variation. We also studied thermal stability of GeO_2. Fig. 4 shows Ge 3d core level spectra of GeO_2/Ge after post deposition anneal (PDA). GeO_2 was clearly desorbed above 500^oC. Fig. 5 shows Ge 3d core level spectra of capped GeO_2/Ge. GeO_2 was not desorbed even above 600^oC and capping Al_2O_3 prevented GeO_2 desorption. Fig. 6 and 7 show C-V characteristics of Al/Al_2O_3/GeO_2/p-Ge MOS capacitor at room temperature and –40^oC. There is no significant frequency dispersion and hysteresis. Dielectric constant of GeO_2 was 5.86 as shown in Fig. 8. Fig. 9 shows the interface state density (Dit) with GeON and GeO_2, and Dit of GeO_2 was improved from GeON. Fig. 10 shows the PDA dependence of Dit of GeO_2. Dit was kept at low $10^{11}cm^{-2}eV^{-1}$ up to 500^oC PDA. Finally, we estimated band offset of GeO_2/Ge. Fig. 11 shows O 1s energy loss spectrum of GeO_2. Fig. 12 shows valence band spectra. Fig. 13 summarized band offset and conduction band offset was 0.84eV. GeO_2 has sufficiently high valence band offset for PMOSFET operation.

(2) Interface self-cleaning in high-k dielectric/InGaAs stack during ALD process: We started from surface chemistry of InGaAs. We utilized Synchrotron Radiation photoemission spectroscopy (SRPES). $In_{0.53}Ga_{0.47}As$ was epitaxially grown on semi-insulating InP substrate by MBE. Fig. 14 shows Ga 3d/In 4d/As 3d core level spectra. In as-received sample, GaOx, InOx and AsOx were grown. After HCl wet cleaning, all native oxides were reduced and As-As bonding appeared. After HCl cleaning and ultrahigh vacuum anneal at 400^oC in SRPES chamber, all native oxides and also surface As-As were gone. Next, we investigated interface property after ALD process. We deposited 10nm-thickHfO_2 intentionally on native oxides of InGaAs to know how native oxides will change after ALD. Then we etched back HfO_2 by dilute HF in Fig. 15. Then we scan indeed the interface of HfO_2/InGaAs. Fig. 16 shows Ga 3d/In 4d/As 3d core level spectra of HfO_2/InGaAs and all native oxides were reduced and interface As-As bonding appeared, which is similar to surface cleaning of InGaAs. Self-cleaning phenomenon is probably attributed to highly reactive chemical process and high formation free energy of native oxides, tabulated in Table. 1. Fig. 17 show the cross sectional TEM images of native oxides and HfO_2 on InGaAs. Native oxide was clearly thinned down after ALD from 2nm to less than 1nm. Fig.

18, 19 shows C-V and I-V characteristics of HfO_2/InGaAs. There was no significant frequency dispersion and hysteresis observed. Finally we also estimated band offset of HfO_2/InGaAs. Fig. 20 and 21 show valence band spectra and O 1s energy loss spectrum, respectively. Fig. 22 summarizes the band offsets and conduction band offset was estimated to be 1.84eV. Therefore HfO2 has sufficiently high conduction band offset and is suitable for NMOSFET operation.

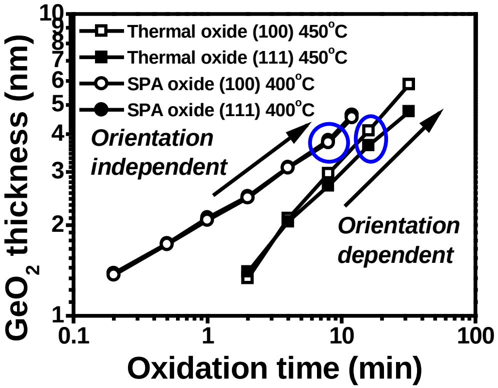

Fig. 1 GeO_2 thickness as a function of oxidation time for thermal oxidation and plasma oxidation on (100) and (111) Ge substrate.

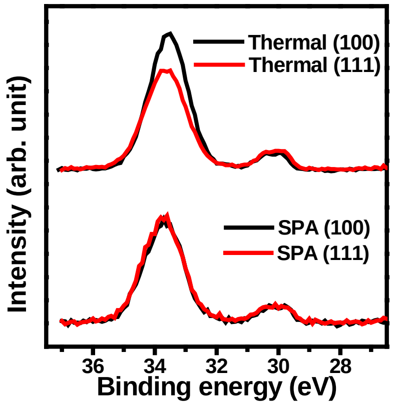

Fig. 2 Ge 3d core level spectra of plasma oxidized and thermally oxidized Ge substrates for marked condition in Fig. 2

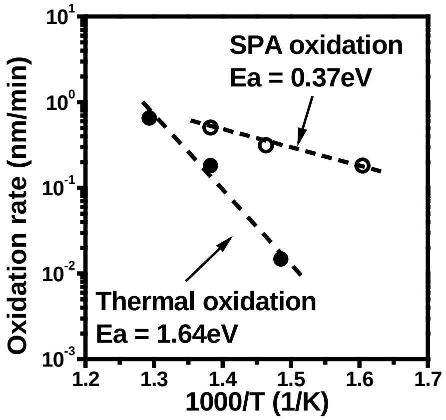

Fig. 3 Ahrrenius plotting of oxidation rate of plasma oxidation and thermal oxidation. Activation energy of SPA oxidation is very low.

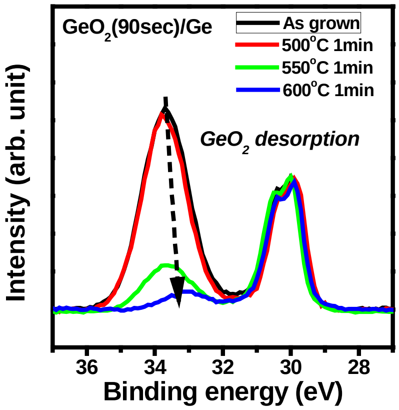

Fig. 4 Ge 3d core level spectra of uncapped GeO_2 on Ge substrate after PDA. Above 550°C, GeO_2 was clearly desorbed from the substrate.

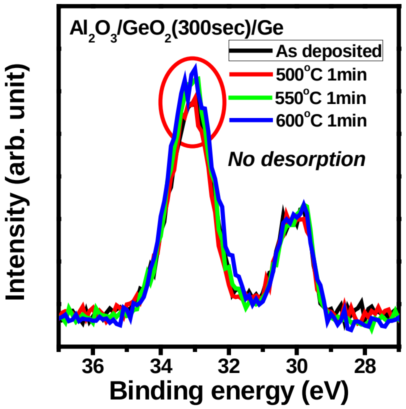

Fig. 5 Ge 3d core level spectra of Al_2O_3 capped GeO_2 on Ge substrate after PDA. Even above 550°C, GeO_2 desorption was well suppressed.

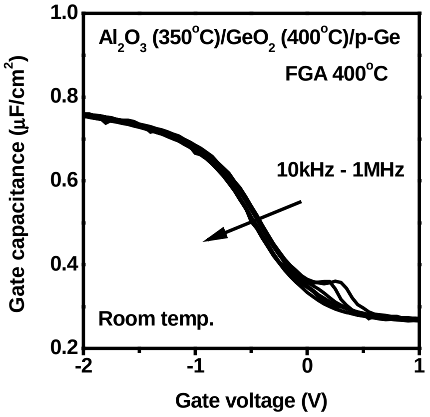

Fig. 6 C-V characteristics of a Al_2O_3/GeO_2/p-Ge MOS capacitor at room temperature for 10kHz, 100kHz, and 1MHz.

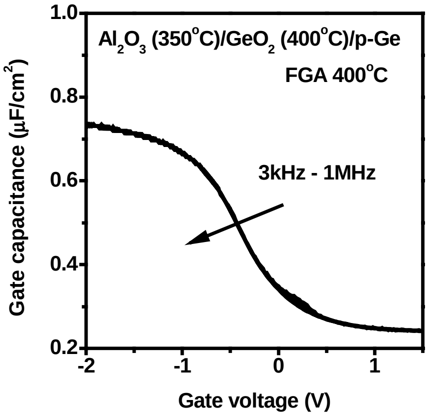

Fig. 7 C-V characteristics of Al_2O_3/GeO_2/p-Ge MOS capacitor at –40°C for 1kHz to 1MHz.

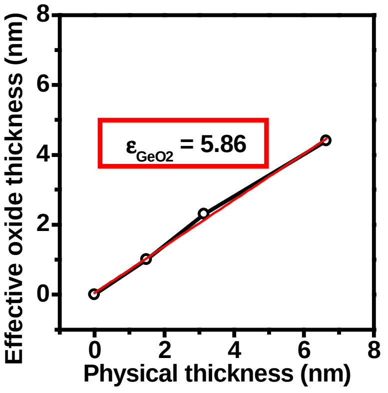

Fig. 8 EOT versus XPS physical oxide thickness, from which dielectric constant of GeO_2 is estimated to be 5.86.

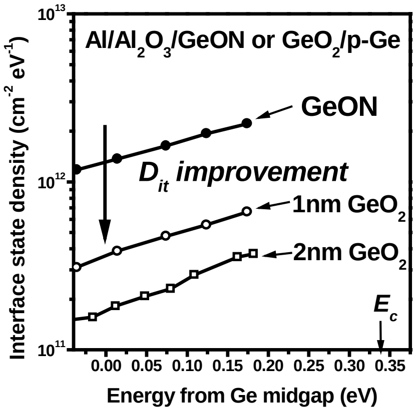

Fig. 9 Inteface state density in upper Ge bandgap for plasma nitridated GeON, and GeO_2. The minimum Dit, 1.4 x $10^{11}cm^{-2}eV^{-1}$ was obtained.

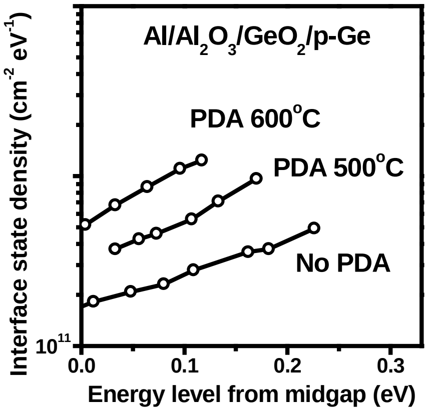

Fig. 10 Fig. 12 Inteface state density in upper Ge bandgap for plasma nitridated GeON, and GeO_2. The minimum D_{it}, 1.4 x 10^{11}cm^{-2}eV^{-1} was obtained.

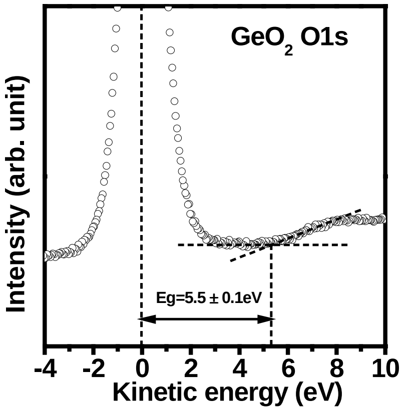

Fig. 11 O 1s energy loss spectrum of GeO_2 on Ge substrate taken with SRPES. Bandgap of GeO_2 was estimated to be 5.3eV.

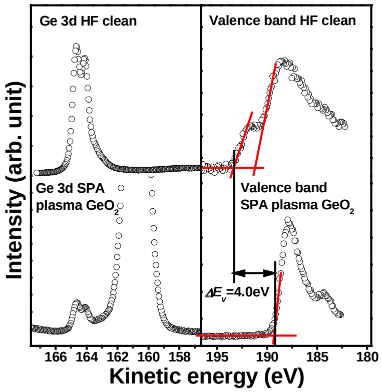

Fig. 12 Ge 3d core level spectra and valence band spectra of clean Ge substrate and GeO_2/Ge. ΔEc and ΔEv of GeO_2/Ge are 0.84eV and 4.0eV.

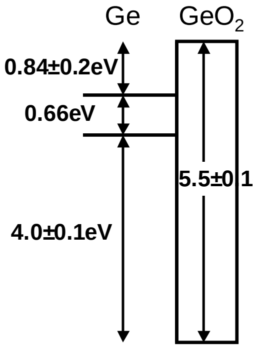

Fig. 13 Band diagram of GeO_2/Ge stack. High tunneling barrier is formed at the valence band.

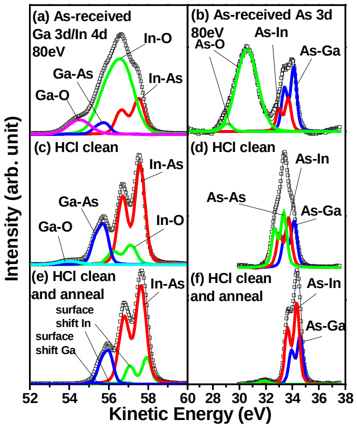

Fig. 14 Ga 3d/In 4d and As 3d spectrum of (a, b) as-received, (c, d) HCl clean, (e, f), HCl clean + annealed, InGaAs substrate.

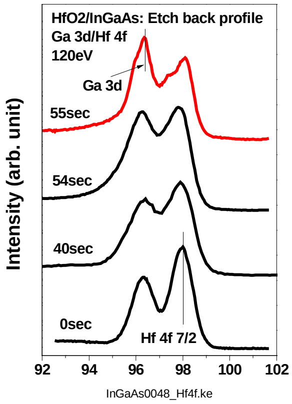

Fig. 15 Etch-back profile of Ga 3d/Hf 4f spectrum of HfO_2/InGaAs.

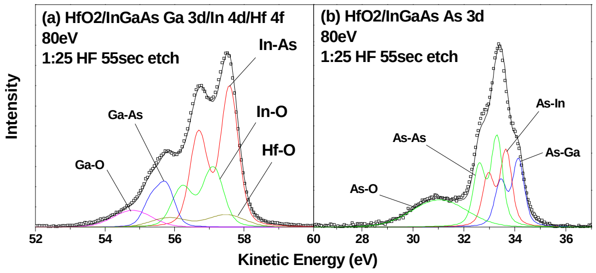

Fig. 16 (a) Ga 3d/In 4d/Hf 4f spectrum at the interface of HfO_2/InGaAs after 55sec etch-back.

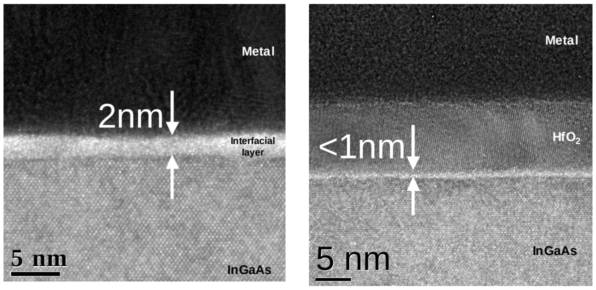

Fig. 17 (Left) Cross sectional TEM image of native oxides on InGaAs. (Right) Cross sectional TEM image of HfO_2 on InGaAs

Table. 1 Standard formation free energy of III-V semiconductors and their oxide.bonding.

III-V semiconductor and oxide	Standard free energy of formation ΔG_f (kcal/mol)
GaAs	-16.01
InAs	-12.81
AlAs	-25.45
As_2O_3	-138
Ga_2O_3	-242.04
In_2O_3	-198.55
Al_2O_3	-378.08
As	3.18

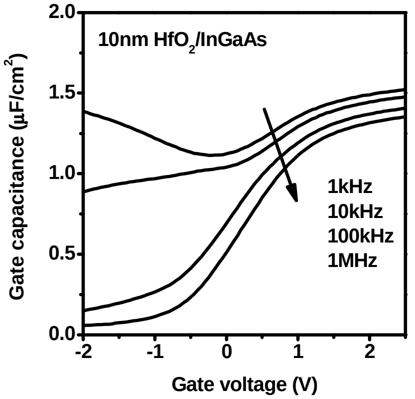

Fig. 18 C-V characteristics of HfO2/InGaAs

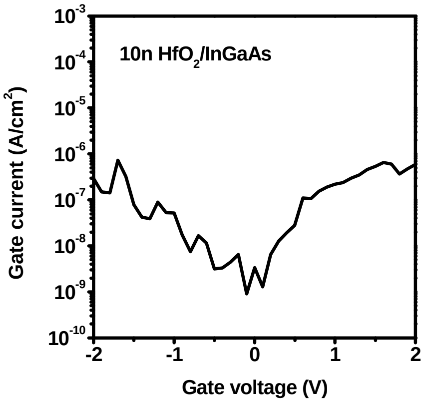

Fig. 19 I-V characteristics of HfO2/InGaAs

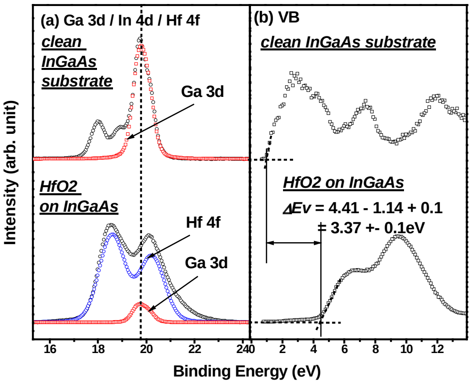

Fig. 20 (a) Ga 3d/In 4d/Hf 4f spectrum after and before etch-back. (b) VB spectrum after and before etch-back.

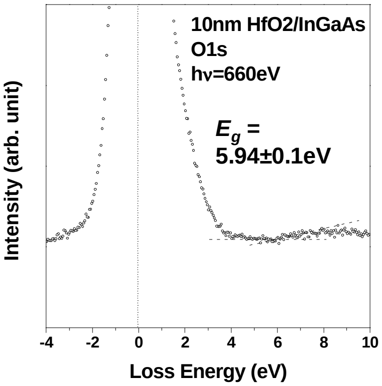

Fig. 21 Oxygen 1s energy loss spectrum of HfO_2/InGaAs.

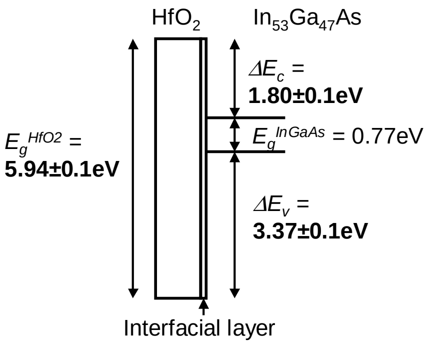

Fig. 22 Experimentally constructed Energy band diagram of HfO_2/InGaAs.